**Atmospheric
Chemistry
and Physics
Discussions**

A comprehensive characterisation of Asian dust storm particles: chemical composition, reactivity to SO$_2$, and hygroscopic property

Q. Ma, Y. Liu, C. Liu, J. Ma, and H. He

State Key Laboratory of Environmental Chemistry and Ecotoxicology, Research Center for Eco-Environmental Sciences, Chinese Academy of Sciences, 18 Shuangqing Road, Haidian District, Beijing 100085, China

Correspondence to: H. He (honghe@rcees.ac.cn)

ACPD

10, 8899–8925, 2010

A comprehensive characterisation of Asian dust storm particles

Q. Ma et al.

Title Page

Abstract	Introduction
Conclusions	References
Tables	Figures

◀ ▶▌

◀ ▶

Back Close

Full Screen / Esc

Printer-friendly Version

Interactive Discussion

Abstract

Mineral dust comprises of a significant fraction of the globe's aerosol loading. Yet it remains the largest uncertainty in future climate predictions due to the complexity in its components and physico-chemical properties. Multi-analysis methods, including SEM-
5 EDX, FTIR, BET, TPD/mass, and Knudsen cell/mass, were used in the present study to characterise Asian dust storm particles. The morphology, element fraction, source distribution, true uptake coefficient of SO_2 and hygroscopic behaviour were studied. The major components of Asian dust storm particles were found to consist of aluminosilicate, SiO_2, and $CaCO_3$, which were coated with organic compounds and inorganic
10 nitrate. The dust storm particles have a low reactivity to SO_2 (true uptake coefficient of 5.767×10^{-6}) which limits the conversion of SO_2 to sulfate during a dust storm period. The low reactivity also demonstrated that the heterogeneous reaction of SO_2, in both dry and humid air conditions, had little effect on the hygroscopic behaviour of the dust particles. These results indicate that the impact of dust storms on atmospheric SO_2
15 removal should not be overestimated.

1 Introduction

Mineral dust is an important and complex constituent of the atmospheric system and influences the Earth's climate and the atmospheric environment in several ways. Firstly, atmospheric mineral dust affects climate directly through the scattering and absorption
20 of solar radiation and indirectly by acting as cloud condensation nuclei (CCN) (Ramanathan et al., 2001). The complexity of the aerosol-cloud-climate system makes the negative forcing, due to atmospheric aerosols, the largest current source of uncertainty in predictions of future global climate (IPCC, 2007). Secondly, mineral dust particles can undergo heterogeneous reactions during atmospheric transportation, altering the
25 chemical balance of the atmosphere and the physiochemical properties of the mineral dust aerosol itself (Cwiertny et al., 2008; Usher et al., 2003). This is significant as

heterogeneous chemical transformations can potentially form dust particles that are more hygroscopic and more efficient CCN (Hanke et al., 2003; Ravishankara, 1997). Finally, cloud processing and heterogeneous chemistry can alter the impact of mineral dust on the ocean biogeochemical cycles (Desboeufs et al., 2001; Hand et al., 2004;

5 Meskhidze et al., 2005). For example, Fe-containing mineral dust deposited into the Earth's oceans can modify bio-productivity and biogeochemical cycles by supplying essential nutrients for phytoplankton (Jickells et al., 2005).

With an annual production estimated at 1000–3000 Tg (Bauer et al., 2004; Ginoux et al., 2001), mineral dust aerosol comprises one of the largest mass fractions of the

10 globe's total aerosol loading. The majority of sources are situated in the arid regions of the Northern Hemisphere, which lie in a broad band that extends from the west coast of North Africa, over the Middle East, Central and South Asia, to China (Prospero et al., 2002). The frequent dust storms that sweep over northern Asia from desert areas of Mongolia and China have become increasingly intense over the last decade (Cyra-

15 noski, 2003; Gong et al., 2003). The increased frequency and intensity of such storms has resulted in the concentration of total suspended particulates (TSP) reaching up to 6000 μg m^{-3} during storm periods (Zhuang et al., 2001). Many Chinese researchers have studied the occurrence, development processes, transportation mechanisms and impact on ambient air quality of sand-dust storms in recent years (Gao et al., 1992;

20 Shi et al., 2005; Xie et al., 2005; Sun et al., 2004a, b; Zhang et al., 1996; Zhang et al., 2003). Zhuang et al. (2001) also reported on the composition, source and size distribution of spring dust storms in China and their effects on the global environment. The physical and chemical characteristics of the aerosols in the air during sand-dust storms have been found to be markedly different from those on days with normal weather, with

25 the ambient aerosol during the sand-dust storms coming primarily from local natural sources (Yang et al., 2002). Little data is available, however, on the heterogeneous reactivity and hygroscopic behaviour of the Asian dust particles. This information is crucial in predicting mineral dust impacts on the climate and atmospheric environment.

Sulfur dioxide (SO$_2$) is the predominant gaseous sulfur containing atmospheric trace

gas. It is released into the troposphere by fossil fuel combustion and volcanic emissions as well as through oxidation of dimethyl sulfide (DMS) and other sulfur compounds of biogenic origin. Numerous field, laboratory and modelling studies have provided convincing evidence that mineral dust plays an important role in the chemistry of sul-
fur dioxide (Dentener et al., 1996; Song and Carmichael, 1999). Field studies have recorded anti-correlations between the concentration of sulfur dioxide and Saharan (Andreae et al., 2003; Hanke et al., 2003) and Chinese (Tang et al., 2004) desert dust loading. A recent field study by Xie et al. (2005), however, showed the conversion rate of SO_2 to sulfate during a dust period was very low due to low relative humidity. Such
findings indicate that further laboratory research is required to determine the reactivity of dust storm particles to SO_2. In addition, sulfate coated on mineral dust plays an important role on the dust's hygroscopic behaviour, and could determine CCN activity, precipitation effect and heterogeneous reactivity of mineral dust to reactive gaseous pollutants. In the present study, the Knudsen cell/mass system was used to investi-
gate the reactivity of dust particles to SO_2, and in situ diffuse reflection infrared Fourior transform spectroscopy (DRIFTS) was used to investigate the hygroscopic behaviour of dust particles. The results obtained from this study will improve our knowledge on the effects of dust storm particles on the atmosphere.

2 Experimental section

2.1 Sampling

Dust particles were collected in a clean jar on the roof of a building (about 20 m high) of the Research Center of Eco-Environmental Sciences, CAS (116.3° E, 39.9° N, Beijing), on 16–17 April 2006, during a heavy dust storm. The size distribution measured by laser size analysis showed that the $d_{0.5}$ of the particles was 20 μm. The BET area
determined from nitrogen adsorption-desorption isotherms at 77 K was 5.43 m^2/g.

2.2 FESEM-EDX analysis

Morphology and element analysis was performed with a high-resolution digital field emission scanning electric microscopy (FE-SEM, SUPERA 55, ZEISS, Germany). The energy dispersive X-ray (EDX) spectrometer was coupled with a circle high-performance In-lens SE detector. The acceleration voltage was 15.0 KeV. The sample was diluted in super-purity water (18 mΩ) with ultrasonic dispersion, and was then deposited on a 3×3 mm^2 Cu substrate and dried in a closed box at room temperature for 12 h. A backscattered electron detector was used to image the samples. A 200×100 μm area of the same sample was quantified and a detection limit of 0.5 atomic% was chosen for quantification purposes.

2.3 TPD characterisation

Desorption of the surface species and decomposition of bulk materials were characterised by a Temperature Program Desorption (TPD) experiment, which was conducted in a tubular reactor coupled with a Mass spectrometer (Hiden, 2000). The carrier gas used was Ar in a flow of 50 mL/min and the temperature rise rate was 20 K/min.

2.4 FTIR/DRIFTS experiments

Infrared (IR) experiments were performed with a Nicolet 6700 (Thermo Nicolet, USA) FT-IR spectroscopy. A DTGS detector in transmission mode was used for particle composition analysis, with the aerosol particles diluted with KBr and pure KBr pellets used as reference. All in situ DRIFTS experiments were conducted in a flow system using an in situ diffuse reflection chamber and a high-sensitivity MCT detector. Typically, the samples (about 13 mg) were finely ground and placed in a ceramic crucible in the in situ chamber. The samples were purged overnight under a flow of dry nitrogen to remove surface water. Mass flow controllers and a sample temperature controller were used to simulate real reaction conditions. The relative humidity (RH) of the stream was

controlled by the addition of a humidified nitrogen flow and was recorded by a hygrometer (CENTER 314, ±2% RH). All in situ DRIFTS experiments were conducted at 300 K and in a total flow of 100 mL/min. All the reported DRIFTS spectra were recorded at a resolution of $4\,cm^{-1}$ for 100 scans.

2.5 Knudsen cell/mass experiments

A Knudsen cell/mass system was used to analyse the gas phase loss due to surface reactions and adsorption, which was described in detailed in a previous paper (Liu et al., 2008). The Knudsen cell consisted of a Teflon-coated reaction chamber with an inlet valve, a sample holder and an escape aperture. The reaction chamber was connected to a quadrupole mass spectrometer (Hiden, HAL 3F PIC). The mass spectrometer was pumped differentially by two turbomolecular pumps (Pfeiffer, $60\,L\,s^{-1}$ and $240\,L\,s^{-1}$) to approximately 10^{-8} Torr.

The particle samples were dispersed evenly on the sample holder with alcohol and were then dried at 393 K for 2 h. The pretreated samples and the reactor chamber were evacuated at 323 K for 6 h to reach a base pressure of approximately 5.0×10^{-7} Torr. After the system was cooled to 300 K, the sample cover was closed. The 2.01% SO_2 gas (balanced with N_2) was introduced into the reactor chamber through a leak valve. The pressure in the reactor was measured using an absolute pressure transducer (BOC Edward). Prior to the experiment initiation, the system was passivated with SO_2 for 150 min to a steady QMS signal since the samples were isolated from the gas by the sample cover. Parameters for the Knudsen reaction chamber can be found in Table 1.

3 Results and discussion

3.1 SEM-EDX analysis

Figure 1 illustrates a typical example of the morphology and X-ray spectrum of the particles deposited on the copper substrate. Particles were generally sharp-edged and

irregular in shape and contained mostly crustal elements such as Si, Al, Fe and Ca. The fractions of two major elements, Al and Si, were less than their crustal abundance, as shown in Table 2. This suggests that both anthropogenic and other source aerosols continuously mix with dust storm particles during transportation. Furthermore, C and

Cl were detected with larger weight fractions than their crustal abundance. The unexpected higher fraction of C possibly originated from the deposition of carbonaceous aerosols during the dust event. The carbonaceous aerosol emissions from biomass burning in China, including bio-fuel combustion, agricultural crop residue burning, and forest and grassland fire, are certainly major contributors to organic aerosols in China

(Streets et al., 2003). Additionally, fine particles coated with carbonaceous species showed a more spherical shape, in agreement with the results of previous TEM research (Shi et al., 2005). The higher than expected Cl concentration may have come from polyvinylchloride plastic in trash and coal burning (Sun et al., 2004a). The amount of sulfur was below the detection limit, which indicates little sulfur species were present

on the particles' surface.

Chemically stable mineral particles are widely considered good indicators of atmospheric movements (Zhang et al., 1996). While no spectral elements unique to Chinese dust source regions exists for use as a real tracer, it is reasonable to expect the ratios of some elements to vary with source area. Several researchers found that Si/Fe, Ca/Fe,

Si/Al, Fe/Al, Mg/Al and Sc/Al could be used to identify the origin of the dust from different areas in China (Sun et al., 2004b; Zhang et al., 1996, 2003). Recently, the ratio of Mg/Al was used as an indicator for determining the contribution of local and non-local sources of airborne particulate pollution at Beijing (Han et al., 2005). In the present study, the ratio of Mg/Al was approximately 0.32. The reference values for the ratio

of Mg/Al are 0.45 for Beijing soil, 0.12 for Duolun in Inner Mongolia (which was the original area of this dust storm), and 0.15 for Fengning, an area between Beijing and Duolun (Han et al., 2005). Due to the uncertainty of energy-dispersive X-ray spectrum, it is not possible to evaluate the contributions of each source accurately. The results do imply, however, that other aerosol sources are continually deposited on the dust

particles during transportation.

3.2 TPD and FTIR experiments

Temperature program desorption is a useful method for surface species analysis in surface science, and was used in the present study to gain insight into the dust particle's major surface components. The desorbed species of CO_2 (m/e=44), H_2O (m/e=18), CO (m/e=28), NO (m/e=30), SO_2 (m/e=64), O_2 (m/e=32), and NO_2 (m/e=46) were monitored by mass spectrometer. As seen from Fig. 2a, four peaks for water (m/e=18) at 362, 423, 643 and 838 K were observed. The results showed that an amount of water was adsorbed on the particles' surface in the ambient atmosphere and some hydroxyl groups were also present on dust particles' surface. During the desorption program, physically adsorbed water molecules desorbed at low temperature and the water from the hydroxyl groups desorbed at high temperature. In addition, another source of water desorbed at high temperature was the oxidation product of organic species adsorbed on the particles (discussed later). The intense desorption peak of CO_2 (m/e=44) with the fraction peak CO (m/e=28) at 976 K was due to the decomposition of calcium carbonate, often reported as a major component of Asian dust particles (Shi et al. 2005; Xie et al., 2005; Zhang et al., 2003). In addition, both the mass signal intensities of CO_2 and CO increased gradually when the temperature was above 540 K, which may be due to the burning of organic species. Although the whole program was in an Ar atmosphere, residual O_2 (m/e=32) was present and was consumed when the temperature was above 540 K, as shown in Fig. 2a. Moreover, the sample turned from brown to black after the TPD process due to the residual black carbon. These results show that many carbonaceous species coated these particles, which was consistent with the higher C weight percentage obtained in the EDX spectrum. Desorption of NO was also observed, indicating the presence of a surface nitrate species. Previous research has shown that atmospheric HNO_3 can be readily adsorbed on mineral dust due to its basicity when the dust contained calcite (Usher et al., 2003). The complete conversion of authentic mineral dust samples, through a heterogeneous reaction between $CaCO_3$

A comprehensive characterisation of Asian dust storm particles

Q. Ma et al.

Title Page

Abstract | Introduction

Conclusions | References

Tables | Figures

|◄ | ►|

◄ | ►

Back | Close

Full Screen / Esc

Printer-friendly Version

Interactive Discussion

and HNO_3, has also been reported in laboratory and field studies (Laskin et al., 2005a, b). These processes resulted in the nitrate-coated dust observed in this study. Our results also showed there was no SO_2 desorption, which was in good agreement with the EDX findings and indicates that there was little sulfur species on the surface of the particles.

The composition of the dust particles was further analysed using Fourier transform infrared (FTIR) spectroscopy to characterise the surface species and the structure of the substrate. The sample was heated in air for 12 h at different temperature (573 and 973 K) to remove different surface species and study the structure information of the substrate. The IR spectra of the fresh sample, as well as the different temperature heated samples, are shown in Fig. 2b. Several bands at 1030, 798, 773, 690 and 472 cm^{-1} were observed in all three samples, which can be attributed to the stretching of Si-O, Si-O-Al and Al-O (Mashburn et al., 2006). This suggests that thermal treatment did not destroy the skeleton structure of the aerosol particle. The bands observed on the fresh sample at 1435, 875 and 525 cm^{-1}, which were also present on the 573 K heated sample, disappeared after being heated at 973 K. The bands at 1435 and 875 cm^{-1} were assigned to asymmetric stretching (v_3) and in-plane bend (v_4) of CO_3^{2-} in calcium carbonate, respectively (Al-Hosney et al., 2005). Since $CaCO_3$ particles, exposed to ambient atmosphere, are terminated by a $Ca(OH)(CO_3H)$ surface layer (Al-Hosney et al., 2005), the peak at 525 cm^{-1} was attributed to v_7 (OC-OH) (Baltrusaitis et al., 2006). These results were in good agreement with the TPD findings, which showed decomposition of $CaCO_3$ at 976 K. The band at 1385 cm^{-1}, which was attributed to H-C bending mode, disappeared after being heated at 573 K. This was due to the oxidation of the organic species, as shown in the TPD results. The peak at 1620 cm^{-1} may be due to the bend mode of H-O-H or the asymmetric stretching (COO) of carboxylic species. The TPD and FTIR results showed that the major components of the dust particles were aluminosilicate, SiO_2 and $CaCO_3$, which were coated with organic species.

3.3 Knudsen cell experiments

The uptake of SO_2 on the dust particles was investigated by a Knudsen cell/Mass system to study its heterogeneous reactivity with mineral dust. Initially, a steady flow of SO_2 was achieved before the powder was exposed. Upon opening the sample
5   holder lid, the parent ion SO_2 signal, monitored at m/e=64, dropped dramatically. The observed uptake coefficient, γ_{obs}, can be determined from the Knudsen cell equation as follows (Golden et al., 1973):

$$\gamma_{obs} = \frac{A_h}{A_s} \frac{I_0 - I}{I} \qquad (1)$$

where A_h is the effective area of the escape hole, or escape aperture (A_h=0.4 mm^2),
10   A_s is the geometric area of the sample holder (A_s=5.26 cm^2), and I_0 and I are the QMS intensities measured with sample covered and sample exposed, respectively. The values calculated in this way are the initial observed uptake coefficients, $\gamma_{0,obs}$, representing the uptake coefficient observed at the initial stages of the reaction. As reported by Usher et al. (2002), the uptake coefficient of SO_2 on mineral oxides de-
15   pends on the sample mass, which has been ascribed to the diffusion of SO_2 into the underlying layers of multilayer powder samples (Underwood et al., 2000). When the uptake coefficient was calculated by Eq. (1), this mass dependence relationship was not considered. However, this must be accounted for in the determination of a true uptake coefficient.
20   As seen in Fig. 3a, the QMS intensity decreased when the sample holder lid was open to the dust particle sample, yet reverted to initial levels after the lid's closure. The observed uptake coefficient, $\gamma_{0,obs}$ (Fig. 3b) was determined using Eq. (1). The dependence of the initial observed uptake coefficient to sample mass is shown in Fig. 4. It is clear that the observed uptake value was dependent on the mass of the sample:
25   as sample mass increased, so did the observed initial uptake coefficient. The plot in Fig. 4 shows only the region where $\gamma_{0,obs}$ is linearly dependent on the mass.

From the plot in Fig. 4, a mass-independent uptake coefficient can be derived as (Carlos-Cuellar et al., 2003)

$$\gamma_{BET} = \text{slope} \cdot \frac{A_s}{S_{BET}} \qquad (2)$$

where slope is the slope of the plot of γ_{obs} versus sample mass in the linear region (mg^{-1}), and S_{BET} is the specific surface area of the particle sample (5.43 m^2/g). It can be seen that the BET-surface-area-corrected value of the initial uptake coefficient, $\gamma_{0,BET}$, was 5.767×10^{-6}. The value is lower than that reported in other studies when other authentic mineral dust particles were used. Usher et al. (2002) investigated the uptake of SO$_2$ on China loess, with the initial uptake coefficient determined to be $(3\pm1) \times 10^{-5}$. The initial uptake coefficient of SO$_2$ on Saharan dust was $(6.6\pm0.8) \times 10^{-5}$ when flow tube was used (Adams et al., 2005). The low uptake coefficient value obtained in this present study was due to the major components, that is, aluminosilicate and SiO$_2$ as shown by EDX, TPD and FTIR results, having low reactivity to SO$_2$. It can also explain the field measurement results that showed the measured ratio of SO$_4^{2-}$ to (SO$_4^{2-}$ +SO$_2$) was very low during dust periods (Xie et al., 2005). Xie et al. (2005) stated that this phenomenon could be explained by the low relative humidity during the dust period. The low uptake coefficient means the low possibility for the first stage of conversion of SO$_2$ to SO$_4^{2-}$. It should be pointed out that the partial pressure of water in the Knudsen cell was less than 10^{-4} Torr, which means the relative humidity was less than 1%. The role of water on the conversion of SO$_2$ to sulfate could not be accounted for in Knudsen cell experiments. Therefore, we applied in situ DRIFTS to study water uptake as well as the role of water on the heterogeneous reaction of SO$_2$ on dust particles.

3.4 Hygroscopic measurement

Adsorption of water vapour onto dust particles was measured at room temperature by means of DRIFTS. The integrated intensity of the O-H stretching region of 2700–

A comprehensive characterisation of Asian dust storm particles

Q. Ma et al.

Title Page

Abstract	Introduction
Conclusions	References
Tables	Figures

◄ | ►
◄ | ►

Back | Close

Full Screen / Esc

Printer-friendly Version

Interactive Discussion

$3700\,\text{cm}^{-1}$ provides a measure of the amount of water on the surface. The peak in this region is a combination of vibrational modes, symmetric stretch at $3400\,\text{cm}^{-1}$ and asymmetric stretch at $3236\,\text{cm}^{-1}$, which were demonstrated as suitably strong to monitor water adsorption on the surface of the particles (Goodman et al., 2001; Gustafsson

5 et al., 2005). Unlike transmission FTIR, DRIFTS shows no linear relation between band intensity and concentration of absorbent. Gaining quantitative information from the spectra is non-trivial since the Beer-Lambert law, used in transmittance, is not applicable. The Kubelka-Munk (K-M) theory can, however, be applied to improve the linearity of the dependence of signal intensity upon concentration (Armaroli et al., 2004;

10 Gustafsson et al., 2005). Figure 5a shows the water adsorption DRIFTS spectra. The isotherms of water uptake on fresh dust and on dust reacted with SO_2 in dry and humid air conditions obtained after applying the K-M function, are shown in Fig. 5b. The effect of reaction with SO_2 on the hygroscopic behaviour of the dust sample, is discussed later.

15 All the isotherms in Fig. 5b exhibit type III characteristics, indicative of a low adsorption enthalpy in the contact layer. In most cases, the two-parameter BET equation with the assumptions of a uniform surface and an infinite number of layers ($n=\infty$) does not fit the experimental data at high relative pressures when the adsorption isotherm rises indefinitely, and an infinite number of layers ($n=\infty$) of adsorbing gas is predicted to

20 build up on the surface. The three-parameter BET equation limits the number of layers of gas adsorbing at high values of P/P_0, which is as follows:

$$V = \frac{V_m c \frac{P}{P_0}}{1 - \frac{P}{P_0}} \frac{1 - (n+1)(\frac{P}{P_0})^n + n(\frac{P}{P_0})^{n+1}}{1 + (c-1)(\frac{P}{P_0}) - c(\frac{P}{P_0})^{n+1}} \tag{3}$$

where V is the volume of gas adsorbed at equilibrium pressure P, V_m is the volume of gas necessary to cover the surface of the adsorbent with a complete monolayer,

25 P_0 is the saturation vapour pressure of the adsorbing gas at the temperature when the adsorption process occurs. The value n is an adjustable parameter given as the

maximum number of layers of the adsorbing gas and is related to the pore size and properties of the adsorbent. As a result, multilayer formation of adsorbing gas is limited to n layers at large values of P/P_0. The parameter c is the temperature-dependent constant related to the enthalpies of adsorption of the first and higher layers through Eq. (4)

$$c = \exp-[\frac{\Delta H_1^0 - \Delta H_2^0}{RT}] \qquad (4)$$

where ΔH_1^0 is the standard enthalpy of adsorption of the first layer, ΔH_2^0 is the standard enthalpy of adsorption on subsequent layers and is taken as the standard enthalpy of condensation, R is the gas constant and T is the temperature in Kelvin.

Curve-fitting software was used to fit the 3-parameter BET equation for the water adsorption isotherm of the fresh dust sample. The result is shown in Fig. 5b with a correlation coefficient $r=0.99$. The fitting result gave fit values for n (27.6), c (1.52) and V_m. With V_m, the integrated K-M area can be converted to layers of water adsorption. On this basis, the one monolayer of water was calculated to have formed at ∼46% RH. The ambient RH is about 20–80%, which means about 1–4 layers of water can be adsorbed on the particle surface.

The DRIFTS studies of SO_2 adsorption on dust particles under dry and humid (50% RH) air conditions were also conducted. After the adsorption processes, the samples were purged by dry N_2 for 1 h to remove the gaseous-phase and physical-adsorbed SO_2, and the spectra were then collected. As shown in Fig. 6a and b, spectra under both dry and humid air conditions showed no absorbance feature of sulfate species, which further confirms the low reactivity of dust particles to SO_2. Only peaks, due to residual adsorbed water, were observed at 1650 and 3600 cm^{-1}. This suggests that the relatively small amount of water adsorbed at ambient RH cannot significantly enhance the conversion of SO_2 to sulfate during the dust storm period. Additionally, the effect of the SO_2 reaction on the hygroscopic behaviour of dust particles was also studied (Fig. 5b). These results showed that the heterogeneous reactions of SO_2 have only a

A comprehensive characterisation of Asian dust storm particles

Q. Ma et al.

slight effect on the hygroscopic properties of dust particles. There are several reasons to explain this phenomenon. Firstly, the major components SiO_2 and aluminosilicate are inactive to SO_2. Secondly, coating with organic species limits the reaction extent of SO_2 with mineral dust. Finally, to convert SO_2 to sulfate on mineral dust, an oxidant,
5 such as H_2O_2, O_3, HNO_3 or NO_2, is needed (Al-Hosney et al., 2005; Li et al., 2006; Ma et al., 2008; Ullerstam et al., 2002, 2003). These factors are, therefore, probably responsible for the limited effect of the SO_2 reaction on the hygroscopic change of dust particles.

4   Conclusions and atmospheric implication

10 Asian dust storms are one of the largest primary sources of global aerosols. The majority of dust storm particles are deposited during transportation, which has a significant effect on the atmospheric environments of the exposed cities. In this study, dust storm particles collected in Beijing were analysed by SEM-EDX, FTIR and TPD experiments. The major components of the dust particles were SiO_2, aluminosilicate and $CaCO_3$,
15 which were coated with certain organic and nitrate species. These particles contained large fractions from both anthropogenic and natural sources after a long transportation. Knudsen cell experiments demonstrated that the observed uptake coefficient showed a linear mass dependence relationship. With a true uptake coefficient of 5.767×10^6, the reactivity to SO_2 was very low. These results suggest that the removal effect of
20 SO_2 by mineral dust during dust storms should not be overestimated. The isotherm of water adsorption on dust particles showed a III-type BET curve, with the monolayer formed at $\sim$46% RH, and only 1–4 layers of water adsorbed at the ambient RH range (20–80%). Adsorbed water molecules show no enhancement effect on the conversion of SO_2 to sulfate species on the dust particles. In addition, the heterogeneous reaction
25 of SO_2 under both dry and humid air conditions had little influence on the hygroscopic behaviour of dust particles.

A comprehensive characterisation of Asian dust storm particles

Q. Ma et al.

References

Adams, J. W., Rodriguez, D., and Cox, R. A.: The uptake of SO_2 on Saharan dust: a flow tube study, Atmos. Chem. Phys., 5, 2679–2689, 2005,
http://www.atmos-chem-phys.net/5/2679/2005/.

Al-Hosney, H. A., and Grassian, V. H.: Water, sulfur dioxide and nitric acid adsorption on calcium carbonate: A transmission and ATR-FTIR study, Phys. Chem. Chem. Phys., 7, 1266–1276, 2005.

Andreae, M. O., Andreae, T. W., Meyerdierks, D., and Thiel, C.: Marine sulfur cycling and the atmospheric aerosol over the springtime North Atlantic, Chemosphere, 52, 1321–1343, 2003.

Armaroli, T., Bécue, T., and Gautier, S.: Diffuse reflection infrared spectroscopy (DRIFTS): Application to the in situ analysis of catalysts, Oil and Gas Science and Technology, 59, 215–237, 2004.

Baltrusaitis, J., Jensen, J. H., and Grassian, V. H.: FTIR Spectroscopy Combined with Isotope Labeling and Quantum Chemical Calculations to Investigate Adsorbed Bicarbonate Formation Following Reaction of Carbon Dioxide with Surface Hydroxyl Groups on Fe_2O_3 and Al_2O_3, J. Phys. Chem. B, 110, 12005–12016, 2006.

Bauer, S. E., Balkanski, Y., Schulz, M., Hauglustaine, D., and Dentener, F.: Global modeling of heterogeneous chemistry on mineral aerosol surfaces: Influence on tropospheric ozone chemistry and comparison to observations, J. Geophys. Res.-Atmos., 109, D02304, doi:10.1029/2003JD003868, 2004.

Carlos-Cuellar, S., Li, P., Christensen, A. P., Krueger, B. J., Burrichter, C., and Grassian, V. H.: Heterogeneous Uptake Kinetics of Volatile Organic Compounds on Oxide Surfaces Using a Knudsen Cell Reactor: Adsorption of Acetic Acid, Formaldehyde, and Methanol on Fe_2O_3, Al_2O_3, and SiO_2, J. Phys. Chem. A, 107, 4250–4261, 2003.

Cwiertny, D. M., Young, M. A., and Grassian, V. H.: Chemistry and Photochemistry of Mineral Dust Aerosol, Annu. Rev. Phys. Chem., 59, 27–51, 2008.

ACPD

10, 8899–8925, 2010

A comprehensive characterisation of Asian dust storm particles

Q. Ma et al.

Title Page	
Abstract	Introduction
Conclusions	References
Tables	Figures

◄	►
◄	►
Back	Close

Full Screen / Esc

Printer-friendly Version

Interactive Discussion

Cyranoski, D.: China plans clean sweep on dust storms, Nature, 421, 101 pp., 2003.

Dentener, F. J., Carmichael, G. R., Zhang, Y., Lelieveld, J., and Crutzen, P. J.: Role of mineral aerosol as a reactive surface in the global troposphere, J. Geophys. Res.-Atmos., 101, 22869–22889, 1996.

Desboeufs, K. V., Losno, R., and Colin, J. L.: Factors influencing aerosol solubility during cloud processes, Atmos. Environ., 35, 3529–3537, 2001.

Gao, Y., Arimoto, R., Zhou, M. Y., Merrill, J. T., and Duce, R. A.: Relationships between the dust concentrations over eastern Asia and the remote North Pacific, J. Geophys. Res.-Atmos., 97, 9867–9872, 1992.

Ginoux, P., Chin, M., Tegen, I., Prospero, J. M., Holben, B., Dubovik, O., and Lin, S.: Sources and distributions of dust aerosols simulated with the GOCART model, J. Geophys. Res.-Atmos., 106, 20255–20273, 2001.

Golden, D. M., Spokes, G. N., and Benson, S. W.: Very Low-Pressure Pyrolysis (VLPP); A Versatile Kinetic Tool, Angew. Chem., 12, 534–546, 1973.

Gong, S. L., Zhang, X. Y., Zhao, T. L., McKendry, I. G., Jaffe, D. A., and Lu, N. M.: Characterization of soil dust aerosol in China and its transport and distribution during 2001 ACE-Asia: 2. Model simulation and validation, J. Geophys. Res.-Atmos., 108, 4262–4284, 2003.

Goodman, A. L., Bernard, E. T., and Grassian, V. H.: Spectroscopic study of nitric acid and water adsorption on oxide particles: Enhanced nitric acid uptake kinetics in the presence of adsorbed water, J. Phys. Chem. A, 105, 6443–6457, 2001.

Gustafsson, R. J., Orlov, A., Badger, C. L., Griffiths, P. T., Cox, R. A., and Lambert, R. M.: A comprehensive evaluation of water uptake on atmospherically relevant mineral surfaces: DRIFT spectroscopy, thermogravimetric analysis and aerosol growth measurements, Atmos. Chem. Phys., 5, 3415–3421, 2005, http://www.atmos-chem-phys.net/5/3415/2005/.

Han, L. H., Zhuang, G. Z., Sun, Y. L., and Wang, Z. F.: Local and non-local sources of airborne particulate pollution at Beijing, Science in China Ser. B Chemistry, 48, 253–264, 2005.

Hand, J. L., Mahowald, N. M., Chen, Y., Siefert, R. L., Luo, C., Subramaniam, A., and Fung, I.: Estimates of atmospheric-processed soluble iron from observations and a global mineral aerosol model: Biogeochemical implications, J. Geophys. Res.-Atmos., 109, D17205, doi:10.1029/2004JD004574, 2004.

Hanke, M., Umann, B., Uecker, J., Arnold, F., and Bunz, H.: Atmospheric measurements of gas-phase HNO_3 and SO_2 using chemical ionization mass spectrometry during the MINATROC

field campaign 2000 on Monte Cimone, Atmos. Chem. Phys., 3, 417–436, 2003, http://www.atmos-chem-phys.net/3/417/2003/.

Intergovernmental Panel on Climate Change (IPCC) (2007), Summary for policymakers, in: Climate Change 2007: The Physical Science Basis. Contribution of Working Group I to the Fourth Assessment Report of the Intergovernmental Panel on Climate Change, edited by: Qin, D., Manning, M., Marquis, M., Averyt, K., Tignor, M., Miller, Jr. H., Chen, Z., Cambridge University Press: New York, 1–18, 2007.

Jickells, T. D., An, Z. S., Andersen, K. K., Baker, A. R., Bergametti, G., Brooks, N., Cao, J. J., Boyd, P. W., Duce, R. A., Hunter, K., Kawahata, H., Kubilay, N., LaRoche, J., Liss, P. S., Mahowald, N., Prospero, J. M., Ridgwell, A. J., Tegen, I. and Torres, R.: Global iron connections between desert dust, ocean biogeochemistry, and climate, Science, 308, 67–71, 2005.

Laskin, A., Iedema, M. J., Ichkovich, A., Graber, E. R., Taraniuk, I., and Rudich, Y.: Direct observation of completely processed calcium carbonate dust particles, Faraday Discuss., 130, 453–468, 2005a.

Laskin, A., Wietsma, T. W., Krueger, B. J., and Grassian, V. H.: Heterogeneous chemistry of individual mineral dust particles with nitric acid: A combined CCSEM/EDX, ESEM, and ICP-MS study, J. Geophys. Res.-Atmos, 110(D10), D10208, doi:10.1029/2004JD005206, 2005b.

Li, L., Chen, Z. M., Zhang, Y. H., Zhu, T., Li, J. L., and Ding, J.: Kinetics and mechanism of heterogeneous oxidation of sulfur dioxide by ozone on surface of calcium carbonate, Atmos. Chem. Phys., 6, 2453–2464, 2006, http://www.atmos-chem-phys.net/6/2453/2006/.

Liu, Y. C., He, H., and Ma, Q. X.: Temperature dependence of the heterogeneous reaction of carbonyl sulfide on magnesium oxide, J. Phys. Chem. A, 112, 2820–2826, 2008.

Ma, Q. X., Liu, Y. C., and He, H.: Synergistic Effect between NO_2 and SO_2 in Their Adsorption and Reaction on γ-Alumina, J. Phys. Chem. A, 112, 6630–6635, 2008.

Mashburn, C. D., Frinak, E. K., and Tolbert, M. A.: Heterogeneous uptake of nitric acid on Na-montmorillonite clay as a function of relative humidity, J. Geophys. Res.-Atmos., 111, D15213, doi:10.1029/2005JD006525, 2006.

Meskhidze, N., Chameides, W. L., and Nenes, A.: Dust and pollution: A recipe for enhanced ocean fertilization? J. Geophys. Res.-Atmos., 110, D03301, doi:10.1029/2004JD005082, 2005.

Prospero, J. M., Ginoux, P., Torres, O., Nicholson, S. E., and Gill, T. E.: Environmental char-

acterization of global sources of atmospheric soil dust identified with the Nimbus 7 Total Ozone Mapping Spectrometer (TOMS) absorbing aerosol product, Rev. Geophys., 40, 1002, doi:10.1029/2000RG000095, 2002.

Ramanathan, V., Crutzen, P. J., Kiehl, J. T., and Rosenfeld, D.: Aerosols, climate, and the hydrological cycle, Science, 294, 2119–2124, 2001.

Ravishankara, A. R.: Heterogeneous and multiphase chemistry in the troposphere, Science, 276, 1058–1065, 1997.

Shi, Z. B., Shao, L. Y., Jones, T. P., and Lu, S. L.: Microscopy and mineralogy of airborne particles collected during severe dust storm episodes in Beijing. China, J. Geophys. Res.-Atmos., 110, D01303, doi:10.1029/2004JD005073, 2005.

Song, C. H., and Carmichael, G. R.: Aging process of naturally emitted aerosol (sea-salt and mineral aerosol) during long range transport, Atmos. Environ., 33, 2203–2218, 1999.

Streets, D. G., Bond, T. C., Carmichael, G. R., Fernandes, S. D., Fu, Q., He, D., Klimont, Z., Nelson, S. M., Tsai, N. Y., Wang, M. Q., Woo, J. -H., and Yarber, K. F.: An inventory of gaseous and primary aerosol emissions in Asia in the year 2000, J. Geophys. Res.-Atmos., 108(D21), 8809, doi:10.1029/2002JD003093, 2003.

Sun, Y. L., Zhuang, G. S., Wang, Y., Han, L. H., Guo, J. H., Dan, M., Zhang, W. J., Wang, Z. F., and Hao, Z. P.: The air-borne particulate pollution in Beijing–concentration, composition, distribution and sources, Atmos. Environ., 38, 5991–6004, 2004a.

Sun, Y. L., Zhuang, G. S., Yuan, H., Zhang, X. Y., and Guo, J. H.: Characteristics and sources of 2002 super dust storm in Beijing, Chinese Science Bulletin, 49, 698–705, 2004b.

Tang, Y. H., Carmichael, G. R., Kurata, G., Uno, I., Weber, R. J., Song, C., Guttikunda, S. K., Woo, J., Streets, D. G., Wei, C., Clarke, A. D., Huebert, B., and Anderson, T. L.: Impacts of dust on regional tropospheric chemistry during the ACE-Asia experiment: A model study with observations, J. Geophys. Res.-Atmos., 109, D19S21, doi:10.1029/2003JD003806, 2004.

Ullerstam, M., Johnson, M. S., Vogt, R., and Ljungström, E.: DRIFTS and Knudsen cell study of the heterogeneous reactivity of SO_2 and NO_2 on mineral dust, Atmos. Chem. Phys., 3, 2043–2051, 2003,
http://www.atmos-chem-phys.net/3/2043/2003/.

Ullerstam, M., Vogt, R., Langer, S., and Ljungström, E.: The kinetics and mechanism of SO_2 oxidation by O_3 on mineral dust, Phys. Chem. Chem. Phys., 4, 4694–4699, 2002.

Underwood, G. M., Li, P., Usher, C. R., and Grassian, V. H.: Determining accurate kinetic parameters of potentially important heterogeneous atmospheric reactions on solid particle

A comprehensive characterisation of Asian dust storm particles

Q. Ma et al.

Full Screen / Esc

Printer-friendly Version

Interactive Discussion

surfaces with a Knudsen cell reactor, J. Phys. Chem. A., 104, 819–829, 2000.

Usher, C. R., Al-Hosney, H., Carlos-Cuellar, S., and Grassian, V. H.: A laboratory study of the heterogeneous uptake and oxidation of sulfur dioxide on mineral dust particles, J. Geophys. Res.-Atmos., 107(D23), 4713, doi:10.1029/2002JD002051, 2002.

Usher, C. R., Michel, A. E., and Grassian, V. H.: Reactions on mineral dust, Chem. Rev., 103, 4883–4940, 2003.

Xie, S. D., Zhang, Y. H., Li, Q., and Tang, X. Y.: Characteristics of air pollution in Beijing during sand-dust storm periods, Water, Air, & Soil Pollution: Focus, 5, 217–229, 2005.

Yang, D. Z., Yan, P., and Xu, X. D.: Characteristics of aerosols under dust and sand weather in Beijing, J. Appl. Meteo. Sci., 13, 185–194, 2002 (in Chinese).

Zhang, X. Y., Gong, S. L., Shen, Z. X., Mei, F., Xi, X., Liu, L., Zhou, Z., Wang, D., Wang, Y., and Cheng, Y.: Characterization of soil dust aerosol in China and its transport and distribution during 2001 ACE-Asia: 1. Network observations, J. Geophys. Res.-Atmos., 108(D9), 8032–8039, 2003.

Zhang, X. Y., Zhang, G. Y., Zhu, G. H., Zhang, D., An, Z. S., Chen, T., and Huang, X. P.: Elemental tracers for Chinese source dust, Science in China (Series D), 39, 512–521, 1996.

Zhuang, G. S., Guo, J. H., Yuan, H., and Zhao, C. Y.: The compositions, sources, and size distribution of the dust storm from China in spring of 2000 and its impact on the global environment, Chinese Science Bulletin, 46, 895–900, 2001.

Title Page

Abstract | Introduction

Conclusions | References

Tables | Figures

◄ | ►

◄ | ►

Back | Close

Full Screen / Esc

Printer-friendly Version

Interactive Discussion

Full Screen / Esc

Table 1. Knudsen reactor parameters.

Knudsen reactor parameter	value
reactor volume, V	94.0±0.5 mL
experimental temperature, T	300±0.1 K
geometric sample area, A_s	5.26±0.05 cm^2
escape orifice area, A_h	0.40±0.03 mm^2
escape rate[a], k_{esc}	1.8 s

[a] calculation from $\ln(\frac{I-I'}{I_0-I'}) \propto t$, I_0, I' and I are the QMS signal intensities of N$_2$ for first steady state, second one and the signal intensities between these two steady states, respectively.

Table 2. FESEM-EDX elements distribution[a].

Element	C	O	Mg	Al	Si	Cl	K	Ca	Fe	S
Weight% Error	22.06±5.09	49.44±1.80	1.80±0.16	5.59±0.23	12.26±0.32	0.78±0.13	1.28±0.15	3.04±0.15	3.75±0.42	n.d.[b]
Crustal abundance	0.003	46.0	1.33	8.04	30.8	0.0001	2.4	3.0	3.5	0.00035
Atom % Error	31.44±7.26	52.89±1.93	1.27±0.11	3.54±0.15	7.47±0.20	0.38±0.06	0.56±0.06	1.30 ±0.10	1.15±0.13	n.d.[b]

[a] Average concentration from 3 measurements. N not detected due to the spectral overlap; [b] n.d. – not detected or below detection limit.

Q. Ma et al.
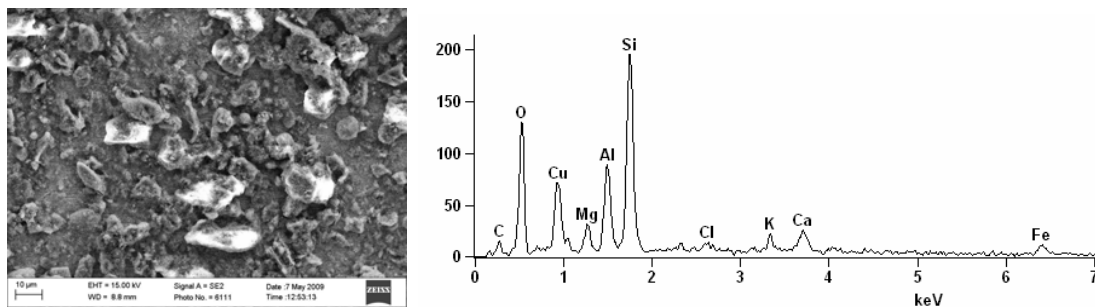
Fig. 1. SEM image of dust particle sample (left) and the EDX spectrum (right).
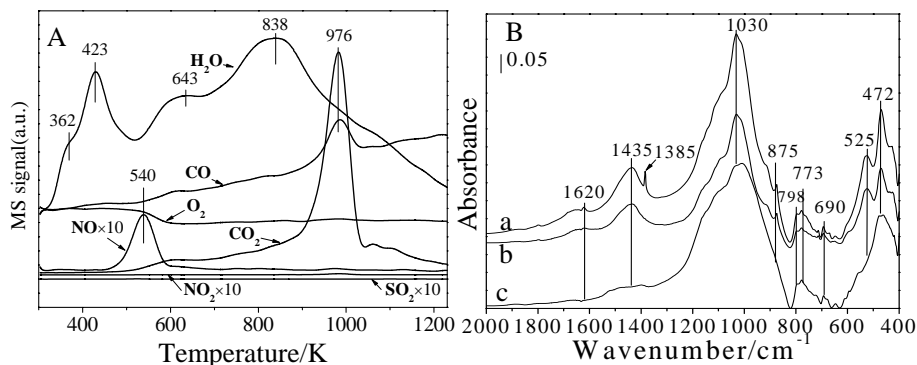
Fig. 2. Characterisation of Asian dust storm particles. **(A)** TPD spectra, condition: carrier gas Ar=50 mL/min, β=20 K/min, m_{sample}=200 mg. **(B)** FTIR spectra of (a) fresh sample, heated in air for 12 h at (b) 573 K, and (c) 973 K.
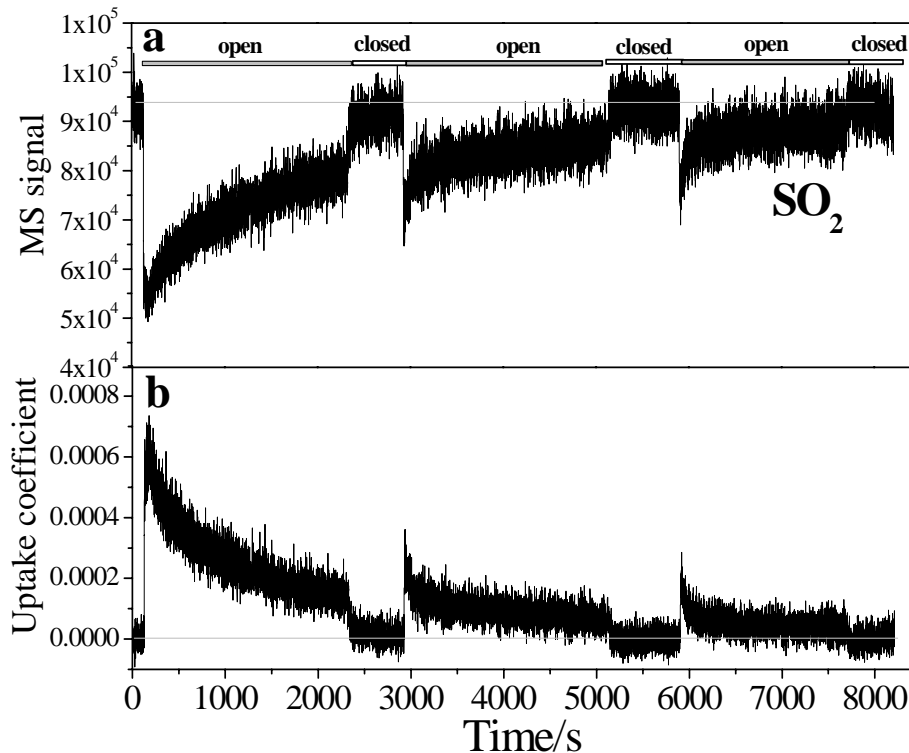
Fig. 3. The uptake of SO_2 on 60 mg dust particle at 300 K. **(a)** the temporal concentration profiles for SO_2 (m/e=64) in the uptake experiment; **(b)** the observed uptake coefficients. Conditions of SO_2 flow: 2.0% in N_2 balance.
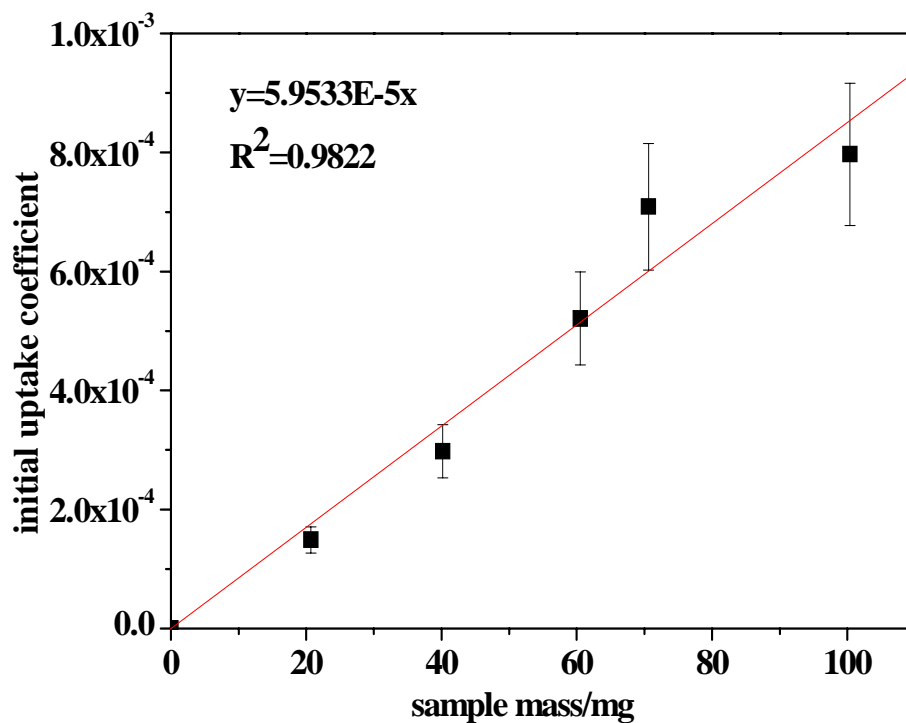
Fig. 4. Linear mass dependence of SO_2 observed uptake coefficients on dust particles at 300 K. Conditions of SO_2 flow: 2.0% in N_2 balance.
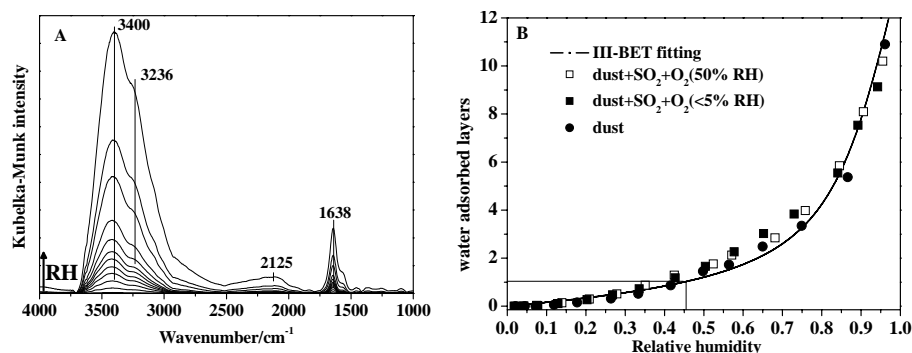
Fig. 5. Water uptake on dust particles obtained at 300 K. **(A)** DRIFTS spectra as a function of RH (2.1, 4.5, 7.2, 11.9, 17.8, 26.4, 33.3, 41.6, 49.8, 56.4, 65.0, 74.9, 86.6, 96.1 %RH); **(B)** isotherms of fresh dust, reacted with SO_2 (200 ppm)+O_2(20%) (<5% RH), and with SO_2 (200 ppm)+O_2 (20%) at RH=50% (50% RH). Integrated region was 2700–3700 cm^{-1}.
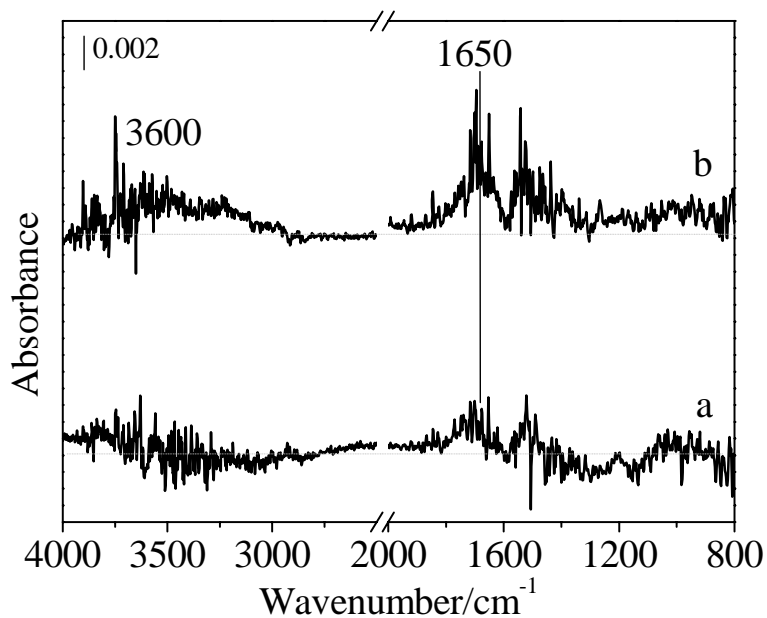
Fig. 6. DRIFTS spectra of SO_2 (200 ppm) adsorption on dust particles in air (20% O_2+N_2) at 300 K for 2 h in **(a)** dry condition and **(b)** humid condition RH=50%.